Journal of Mathematical Chemistry 4(1990)117–126

EIGENVALUE CORRELATION DIAGRAMS FOR EFFECTIVE HAMILTONIANS: THE ESR SPECTRUM OF AXIAL Gd(III)

M.L. ELLZEY, Jr.
Department of Chemistry, The University of Texas, El Paso, Texas 79968–0512, USA

Abstract

Correlation diagrams depicting the behavior of effective Hamiltonian eigenvalues over the ranges of its variables may reveal important properties of the models. The case in which a Hamiltonian is a sum of two terms, one going to zero in one limit and the other effectively zero in the other limit, is considered here. The electron spin resonance spectrum calculated from the spin Hamiltonian of axial gadolinium III is used here as an example. The zero-field splitting term of the spin Hamiltonian is expanded in terms of normalized irreducible tensorial matrices in order to take advantage of their transformation properties under rotations. Its eigenvalues are plotted in a correlation diagram from the zero-field to the high-field limit. A similar correlation diagram for the principal transitions is used to predict a resonance spectrum.

1. Introduction

Energy level correlation diagrams are commonly employed in quantum chemistry. For example, Tanabe and Sugano use energy level correlation diagrams [1] to illustrate the effect of a crystal field on atomic multiplets, although the nonlinear plots of Matsen and Ellzey [2] actually include the limits. Correlation diagrams for eigenvalues of effective Hamiltonians which are sums of two competing terms – each dominating in different limits – are considered here.

Effective Hamiltonian techniques are well established in the spin-Hamiltonian analysis of electron spin resonance spectroscopy [3]. Not as common in ESR studies, but potentially useful, are energy level correlation diagrams extending from zero magnetic field strength to the high-field limit. As an example, the zero-field splitting of spin levels observed in electron spin resonance spectra of axially symmetric gadolinium III ions is treated here. Symmetry considerations are efficiently realized by expanding the zero-field splitting portion of the spin Hamiltonian in terms of normalized irreducible tensorial matrices (NITM) [4].

This example fits the model of the effective Hamiltonian with two competing terms: one the Zeeman magnetic splitting term and the other a zero-field splitting operator. With this model as a guide, an eigenvalue correlation diagram is constructed for an operator which is the sum of two appropriate operators.

An ESR spectrum is obtained by varying a magnetic field from zero to some large value while maintaining an oscillating field. Resonances occur as the Zeeman splitting

causes differences between energy levels to match the $h\nu$ of the oscillating field. The zero-field splitting is a result of the environment of the magnetic center.

Constant energy quantities, such as the $h\nu$ of the oscillating field, can be indicated on the diagram by taking them to be proportional to the zero-field splitting strength. For the strictly axial model considered here, m_s is an exact quantum number and the selection rule $\Delta m_s = \pm 1$ holds. By plotting an appropriate function corresponding to the resonance field energy, an ESR spectrum is predicted.

2. General correlations

Consider an effective Hamiltonian which can be written as the sum of two terms

$$\boldsymbol{H} = u\boldsymbol{O} + v\boldsymbol{P}, \tag{2.1}$$

where $\boldsymbol{O}$ and $\boldsymbol{P}$ are linear Hermitian operators, and u and v are real scalars corresponding to physical quantities.

There are generally three situations of interest: (1) v negligible with respect to u, (2) u comparable to v, and (3) u negligible with respect to v. To make the diagram independent of the parameter values, energy levels may be plotted as multiples of u in case (1) and as multiples of v in case (2). Dividing eq. (2.1) by u gives

$$\boldsymbol{H}/u = \boldsymbol{O} + (u/v)\boldsymbol{P}. \tag{2.2}$$

The eigenvalues of (2.2) are the energies divided by u, and may be plotted against $(u/v) = 0$ to 1. Dividing (2.1) by v yields

$$\boldsymbol{H}/v = (v/u)\,\boldsymbol{O} + \boldsymbol{P}. \tag{2.3}$$

The eigenvalues of (2.3) are the energies divided by v, and may be plotted against $(v/u) = 1$ to 0. Note that $u = v$ at $(u/v) = (v/u) = 1$. The complete correlation diagram is constructed in this way.

The eigenvalues of $\boldsymbol{H}/u$ or $\boldsymbol{H}/v$ are not linear functions of (u/v) or (v/u) unless both $\boldsymbol{O}$ and $\boldsymbol{P}$ are diagonal. Even then, the slopes of the lines at $(u/v) = (v/u) = 1$ are usually not continuous due to the change from E/u to E/v.

In contrast, a correlation diagram generated by plotting the eigenvalues of the operator [5]

$$\boldsymbol{H}' = x\boldsymbol{O} + (1 - x)\boldsymbol{P} \tag{2.4}$$

as functions of $x = 0$ to 1 does not exhibit these discontinuities, yet the same values are included. Plots against x of the eigenvalues of $\boldsymbol{H}'$ are straight lines if both $\boldsymbol{O}$ and $\boldsymbol{P}$ are diagonal. Graphing is then a simple matter of using a straight edge to connect the eigenvalues of $\boldsymbol{P}$ on the left with the eigenvalues of $\boldsymbol{O}$ on the right.

Despite the different appearances of the correlation diagrams of $\boldsymbol{H}$ and $\boldsymbol{H}'$, they are simply related. For those values of u and υ such that

$$u + \upsilon \neq 0, \tag{2.5}$$

the transformation to $\boldsymbol{H}'$ is given by

$$\boldsymbol{H}' = \boldsymbol{H}/(u + \upsilon), \tag{2.6}$$

$$x = u/(u + \upsilon), \tag{2.7}$$

$$(1 - x) = \upsilon/(u + \upsilon), \tag{2.8}$$

and the reverse is

$$\boldsymbol{H}/u = \boldsymbol{H}'/x, \tag{2.9}$$

$$\boldsymbol{H}/\upsilon = \boldsymbol{H}'/(1 - x), \tag{2.10}$$

$$u/\upsilon = x/(1 - x). \tag{2.11}$$

3. Spin Hamiltonian of Gd(III)

The ground multiplet of gadolinium III is $f^7{:}^8S_{7/2}$, with seven unpaired f electrons and total spin $S = 7/2$. The conventional model for the ESR spectrum of Gd(III) incorporates zero-field splitting but no hyperfine interaction [6] so that the spin Hamiltonian is an eight-by-eight effective Hamiltonian matrix over the eight spin-7/2 states. Then

$$[\boldsymbol{H}] = [\boldsymbol{H}_{\text{Zeeman}}] + [\boldsymbol{H}_{\text{zfs}}], \tag{3.1}$$

where $[\boldsymbol{H}_{\text{Zeeman}}]$ is the Zeeman term given by

$$[\boldsymbol{H}_{\text{Zeeman}}] = \beta \boldsymbol{B} \cdot \boldsymbol{g} \cdot [\boldsymbol{S}], \tag{3.2}$$

with β the Bohr magneton, $\boldsymbol{B}$ the magnetic field, $\boldsymbol{g}$ the g-tensor and $[\boldsymbol{S}]$ the spin vector matrix. The zero-field splitting term $[\boldsymbol{H}_{\text{zfs}}]$ is not zero when $\boldsymbol{B}$ is zero, hence the name. The spin energy levels which would be degenerate in the absence of a magnetic field are split into Kramers doublets [7] by the environment of the Gd(III) ion.

The entire eight-by-eight spin Hamiltonian can be expanded in terms of irreducible tensorial operators [8]. For convenience, the 64 normalized irreducible tensorial matrices [4] $[\boldsymbol{n}_q^{(k)}]^{7/2}$, $k = 0, 1, \ldots, 7$; $q = -k, -k + 1, \ldots, k$, are used here. Their elements are defined in terms of $3j$ symbols [9] according to

$$\langle (3.5)m_1 | \boldsymbol{n}_q^{(k)} | (3.5)m_2 \rangle = (-1)^{(3.5)-m_1} \times \sqrt{2k+1} \begin{pmatrix} 3.5 & k & 3.5 \\ -m_1 & q & m_2 \end{pmatrix}. \tag{3.3}$$

Nonzero elements of these matrices are tabulated in table 1 for $q \geq 0$. Values for negative q are obtained using the relation

$$[\boldsymbol{n}_{-q}^{(k)}]_{mm'} = (-1)^{-q} [\boldsymbol{n}_q^{(k)}]_{m'm}. \tag{3.4}$$

By the Wigner–Eckart theorem, the NITM are irreducible tensorial operators with reduced matrix elements given by

$$\langle S \| \boldsymbol{n}^{(k)} \| S \rangle = \sqrt{2k+1}, \tag{3.5}$$

which ensures the orthonormality relations

$$\text{trace}([\boldsymbol{n}_q^{(k)}]^{\mathrm{T}} [\boldsymbol{n}_{q'}^{(k')}]) = \delta(k,k')\,\delta(q,q'), \tag{3.6}$$

where T indicates the transpose. It follows that the expansion coefficients in

$$[\boldsymbol{H}] = \sum_{k}^{7} \sum_{q} B_q^{(k)} [\boldsymbol{n}_q^{(k)}] \tag{3.7}$$

are given by

$$B_q^{(k)} = \text{trace}([\boldsymbol{n}_q^{(k)}]^{\mathrm{T}} [\boldsymbol{H}]). \tag{3.8}$$

Since the spin operators correspond to a $k = 1$ tensorial set, the coefficients $B_q^{(1)}$ will include the Zeeman contribution to this spin Hamiltonian. If Kramers degeneracy is not lifted by the zero-field splitting, only terms with even k can occur in its expansion

$$[\boldsymbol{H}_{\text{zfs}}] = \sum_{\text{even } k}^{6} \sum_{q} B_q^{(k)} [\boldsymbol{n}_q^{(k)}]. \tag{3.9}$$

Consequently, it is convenient to use expression (3.2) for the Zeeman term and (3.9) for the zero-field splitting. Originally, expansions used in electron spin resonance studies employed Stevens [10] operators, although Buckmaster introduced "Racah" operators [11]. Both are irreducible tensorial operators, differing from the NITM only in their reduced matrix elements. Differences with this work will therefore be in scaling of the parameters.

Table 1

Nonzero elements of $j = 3.5$ normalized irreducible tensorial matrices $[n_q^{(k)}]$ for $q \geq 0$. Values for negative q are obtained from the relation $[n_{-q}^{(k)}]_{mm'} = (-1)^{-q}[n_q^{(k)}]_{m'm}$. Each entry is to be divided by the quantity N at the top of its column

k	0	1	2	3	4	5	6	7	m	m'	q
N	$2\sqrt{2}$	$2\sqrt{42}$	$2\sqrt{42}$	$2\sqrt{66}$	$2\sqrt{154}$	$2\sqrt{546}$	$2\sqrt{66}$	$2\sqrt{858}$			
	1	−7	7	−7	7	−7	1	−1	−3.5	−3.5	
	1	−5	1	5	−13	23	−5	7	−2.5	−2.5	
	1	−3	−3	7	−3	−17	9	−21	−1.5	−1.5	
	1	−1	−5	3	9	−15	−5	35	−0.5	−0.5	0
	1	1	−5	−3	9	15	−5	−35	0.5	0.5	
	1	3	−3	−7	−3	17	9	21	1.5	1.5	
	1	5	1	−5	−13	−23	−5	−7	2.5	2.5	
	1	7	7	7	7	7	1	1	3.5	3.5	
N		$2\sqrt{21}$	$2\sqrt{21}$	$\sqrt{66}$	$\sqrt{154}$	$2\sqrt{273}$	$2\sqrt{33}$	$\sqrt{429}$			
		$-\sqrt{7}$	$\sqrt{21}$	$-\sqrt{21}$	$\sqrt{35}$	$-\sqrt{105}$	$\sqrt{3}$	−1	−2.5	−3.5	
		$-2\sqrt{3}$	4	−1	$-\sqrt{15}$	$8\sqrt{5}$	$-2\sqrt{7}$	$\sqrt{21}$	−1.5	−2.5	
		$-\sqrt{15}$	$\sqrt{5}$	$\sqrt{5}$	$-3\sqrt{3}$	−1	$\sqrt{35}$	$-\sqrt{105}$	−0.5	−1.5	
		−4	0	$2\sqrt{3}$	0	$-4\sqrt{15}$	0	$5\sqrt{7}$	0.5	−0.5	1
		$-\sqrt{15}$	$-\sqrt{5}$	$\sqrt{5}$	$3\sqrt{3}$	−1	$-\sqrt{35}$	$-\sqrt{105}$	1.5	0.5	
		$-2\sqrt{3}$	−4	−1	$\sqrt{15}$	$8\sqrt{5}$	$2\sqrt{7}$	$\sqrt{21}$	2.5	1.5	
		$-\sqrt{7}$	$-\sqrt{21}$	$-\sqrt{21}$	$-\sqrt{35}$	$-\sqrt{105}$	$-\sqrt{3}$	−1	3.5	2.5	
N			$2\sqrt{21}$	$2\sqrt{33}$	$2\sqrt{77}$	$2\sqrt{39}$	$\sqrt{66}$	$\sqrt{286}$			
			$\sqrt{7}$	$-\sqrt{35}$	$\sqrt{105}$	$-\sqrt{35}$	$\sqrt{5}$	$-\sqrt{3}$	−1.5	−3.5	
			$\sqrt{15}$	$-3\sqrt{3}$	1	$3\sqrt{3}$	$-\sqrt{21}$	$\sqrt{35}$	−0.5	−2.5	
			$2\sqrt{5}$	−2	$-4\sqrt{3}$	4	$\sqrt{7}$	$-\sqrt{105}$	0.5	−1.5	2
			$2\sqrt{5}$	2	$-4\sqrt{3}$	−4	$\sqrt{7}$	$\sqrt{105}$	1.5	−0.5	
			$\sqrt{15}$	$3\sqrt{3}$	1	$-3\sqrt{3}$	$-\sqrt{21}$	$-\sqrt{35}$	2.5	0.5	
			$\sqrt{7}$	$\sqrt{35}$	$\sqrt{105}$	$\sqrt{35}$	$\sqrt{5}$	$\sqrt{3}$	3.5	1.5	
N				$\sqrt{66}$	$\sqrt{22}$	$\sqrt{78}$	$\sqrt{22}$	$\sqrt{143}$			
				$-\sqrt{7}$	$\sqrt{7}$	$-2\sqrt{7}$	2	$-\sqrt{5}$	−0.5	−3.5	
				−4	2	1	$-\sqrt{7}$	$\sqrt{35}$	0.5	−2.5	
				$-2\sqrt{5}$	0	$2\sqrt{5}$	0	$-3\sqrt{7}$	1.5	−1.5	3
				−4	−2	1	$\sqrt{7}$	$\sqrt{35}$	2.5	−0.5	
				$-\sqrt{7}$	$-\sqrt{7}$	$-2\sqrt{7}$	−2	$-\sqrt{5}$	3.5	0.5	
N					$2\sqrt{11}$	$2\sqrt{13}$	$2\sqrt{11}$	$2\sqrt{13}$			
					$\sqrt{7}$	$-\sqrt{21}$	$\sqrt{15}$	$-\sqrt{5}$	0.5	3.5	
					$\sqrt{15}$	$-\sqrt{5}$	$-\sqrt{7}$	$\sqrt{21}$	1.5	−2.5	4
					$\sqrt{15}$	$\sqrt{5}$	$-\sqrt{7}$	$-\sqrt{21}$	2.5	−1.5	
					$\sqrt{7}$	$\sqrt{21}$	$\sqrt{15}$	$\sqrt{5}$	3.5	−0.5	
N						$\sqrt{26}$	$\sqrt{2}$	$\sqrt{13}$			
						$-\sqrt{7}$	1	$-\sqrt{3}$	1.5	−3.5	
						$-2\sqrt{3}$	0	$\sqrt{7}$	2.5	−2.5	5
						$-\sqrt{7}$	−1	$-\sqrt{3}$	3.5	−1.5	
N							$\sqrt{2}$	$\sqrt{2}$			
							1	−1	2.5	−3.5	6
							1	1	3.5	−2.5	
N								1			
								−1	3.5	−3.5	7

4. Axial fields

If the symmetry of the zero-field splitting term is axial as, for example, if the ion were embedded between two infinite plates, then $[\boldsymbol{H}_{zfs}]$ must commute with all rotations about the high symmetry axis. The NITMs transform under rotations according to the Wigner–Racah rotation matrices [12] so that by taking the high symmetry axis to be the z-axis, only those tensors with $q = 0$ will remain in the expansion of $[\boldsymbol{H}_{zfs}]$. Since from table 1 each NITM with $q = 0$ is diagonal, the entire zero-field splitting Hamiltonian is diagonal.

For axial systems, the g-tensor is diagonalized to the terms g_{zz} and $g_{xx} = g_{yy}$. In the strictly axial model, the high symmetry z-axis of the g-tensor coincides with the z-axis of the zero-field splitting term. Taking $\boldsymbol{B}$ along the z-axis in the Zeeman term then

$$[\boldsymbol{H}] = \beta g_{zz} B_z [S_z] + B_0^{(2)}[\boldsymbol{n}_0^{(2)}] + B_0^{(4)}[\boldsymbol{n}_0^{(4)}] + B_0^{(6)}[\boldsymbol{n}_0^{(6)}]. \tag{4.1}$$

This simple model is not entirely unrealistic and the correlation curves are linear and easy to plot, yielding insight with minimal effort. This operator can be further simplified by taking into account the normalization factors in table 1,

$$[\boldsymbol{H}] = Z(2[S_z]) + b(2)[\boldsymbol{P}], \tag{4.2}$$

where

$$[\boldsymbol{P}] = [\boldsymbol{n}_0^{(2)}] + \{b(4)/b(2)\}[\boldsymbol{n}_0^{(4)}] + \{b(6)/b(2)\}[\boldsymbol{n}_0^{(6)}], \tag{4.3}$$

$$Z = \beta g_{zz} B_z / 2, \tag{4.4}$$

$$b(2) = B_0^{(2)}/(2\sqrt{42}), \tag{4.5}$$

$$b(4) = B_0^{(4)}/(2\sqrt{154}), \tag{4.6}$$

$$b(6) = B_0^{(6)}/(2\sqrt{66}). \tag{4.7}$$

The factor of 2 multiplying $[S_z]$ is included for convenience in order to avoid the half-integer eigenvalues of $[S_z]$.

5. Energy correlation diagram for axial fields

The energy level correlation diagram is generated by graphing the eigenvalues of the operator

$$[\boldsymbol{H}'] = x(2[S_z]) + (1-x)[\boldsymbol{P}] \tag{5.1}$$

as functions of $x = 0$ to 1. Since both $2[S_z]$ and $[P]$ are diagonal, the eigenvalues are the diagonal elements given by

m_s	$E'(m_s)$
−7/2	$x(-7) + (1-x)\,W(7)$,
−5/2	$x(-5) + (1-x)\,W(5)$,
−3/2	$x(-3) + (1-x)\,W(3)$,
−1/2	$x(-1) + (1-x)\,W(1)$,
1/2	$x(1) + (1-x)\,W(1)$,
3/2	$x(3) + (1-x)\,W(3)$,
5/2	$x(5) + (1-x)\,W(5)$,
7/2	$x(7) + (1-x)\,W(7)$,

(5.2)

where the W quantities are the diagonal elements of $[P]$ and are obtained from table 1 and the definition of $[P]$ in (4.3):

$$\begin{aligned} W(1) &= -5 + 9(b(4)/b(2)) - 5(b(6)/b(2)), \\ W(3) &= -3 - 3(b(4)/b(2)) + 9(b(6)/b(2)), \\ W(5) &= 1 - 13(b(4)/b(2)) - 5(b(6)/b(2)), \\ W(7) &= 7 + 7(b(4)/b(2)) + (b(6)/b(2)). \end{aligned} \tag{5.3}$$

Assigning arbitrary, but reasonable, values of 0.05 and 0.008 to the ratios $b(4)/b(2)$ and $b(6)/b(2)$ gives W values of

$$\begin{aligned} W(1) &= -4.59, \\ W(3) &= -3.08, \\ W(5) &= 0.31, \\ W(7) &= 7.36. \end{aligned} \tag{5.4}$$

These eigenvalues of $[P]$ are the intercepts on the $x = 0$ side of the correlation diagram depicted in fig. 1. The intercepts on the right-hand side of fig. 1 are the eigenvalues of $2[S_z]$.

Since m_s is a good quantum number throughout this correlation, the selection rule $\Delta m_s = \pm 1$ holds for transitions. The seven differences $E(m_s + 1) - E(m_s)$ obtained from (5.2) are

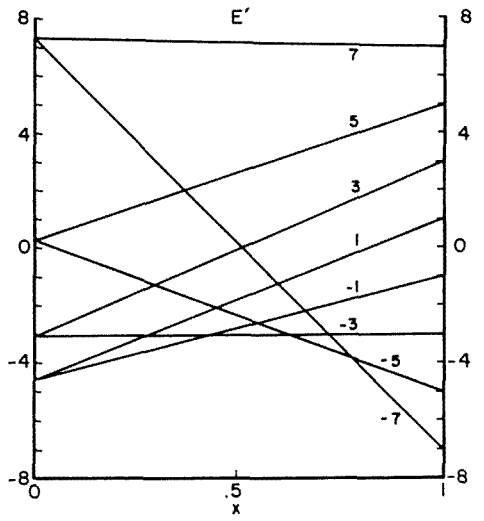

Fig. 1. Plot of eigenvalues of $[H'] = x(2[S_z]) + (1 - x)[P]$ versus x, where $[P]$ is defined in eq. (4.2). The formulas for these functions are given in eq. (5.2). For this display, $b(4)/b(2) = 0.05$ and $b(6)/b(2) = 0.008$. The levels are identified by their right-hand side intercepts $2m_s$.

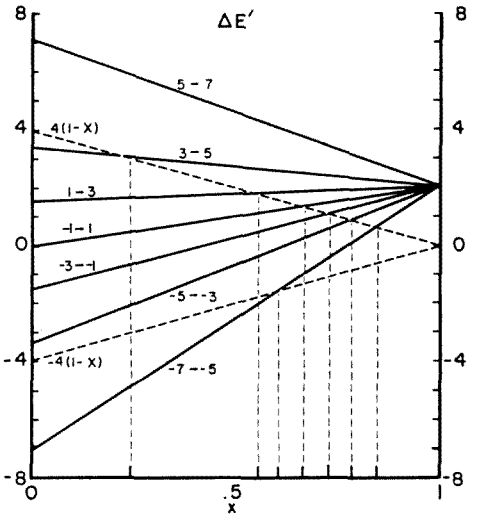

Fig. 2. Plot of the differences $\Delta E' = E'(m_s + 1) - E'(m_s)$ of the eigenvalues of $[H'] = x(2[S_z]) + (1 - x)[P]$. The values and ranges of all variables are the same as in fig. 1. For convenience, the eigenvalues are identified by $2m_s$. The dotted lines represent the values $\pm 4(1 - x)$ corresponding to hypothetical resonance energies of $h\nu = \pm 4b(2)$ for an ESR spectrum. Resonance lines occurring where the energy differences are equal to these values are shown along the bottom axis. Note that this spectrum is independent of the sign of the zero-field splitting.

Transition	$\Delta E'$
$-7/2 \rightarrow -5/2$	$x + (1 - x)\{W(5) - W(7)\}$,
$-5/2 \rightarrow -3/2$	$x + (1 - x)\{W(3) - W(5)\}$,
$-3/2 \rightarrow -1/2$	$x + (1 - x)\{W(1) - W(3)\}$,
$-1/2 \rightarrow 1/2$	$x + (1 - x)\{W(1) - W(1)\}$,
$1/2 \rightarrow 3/2$	$x + (1 - x)\{W(3) - W(1)\}$,
$3/2 \rightarrow 5/2$	$x + (1 - x)\{W(5) - W(3)\}$,
$5/2 \rightarrow 7/2$	$x + (1 - x)\{W(7) - W(5)\}$.

(5.5)

These are plotted in fig. 2 between the same limits as fig. 1. The negative values are an artifact of this method since, for example, the $m_s = -7/2$ level is actually above the $m_s = -5/2$ level until high fields.

6. Electron spin resonance correlation diagrams

For ESR purposes, the magnetic field is increased from zero, inducing resonance as various energy level differences, consistent with any selection rules, become equal to the $h\nu$ of an oscillating magnetic field perpendicular to $\boldsymbol{B}$. By definition (4.4), the parameter Z is proportional to the field strength B_z and varies accordingly. The zero-field splitting parameter $b(2)$, however, is a constant for a particular system.

In order to interpret the energy level correlation diagrams in figs. 1 and 2 for electron spin resonance spectroscopy, eq. (5.1) is compared to eq. (4.2). Assuming $Z + b(2) \neq 0$, which is valid for all Z if $b(2) > 0$, the quantities are related by

$$[\boldsymbol{H}'] = [\boldsymbol{H}]/(Z + b(2)) \tag{6.1}$$

and

$$x = Z/(Z + b(2)). \tag{6.2}$$

The variation of x from 0 to 1 therefore corresponds to the variation of Z from 0 to infinity. A negative value of $b(2)$ can be handled by changing the sign of $[\boldsymbol{P}]$.

It is convenient to specify energy quantities in units of the constant $b(2)$. For example, if a particular value of Z is $Z = kb(2)$, then the corresponding value of x is $x = k/(1 + k)$. The energies of the original spin Hamiltonian in units of $b(2)$ are given in terms of $[\boldsymbol{H}']$ and x by

$$[\boldsymbol{H}]/b(2) = [\boldsymbol{H}']/(1 - x). \tag{6.3}$$

A constant energy $E_c = cb(2)$ becomes the straight line $E' = c(1 - x)$. In fig. 2, dashed lines $\Delta E' = \pm 4(1 - x)$ corresponding to $\Delta E = \pm 4b(2)$ are displayed. A resonance would be observed at a value of x for which a transition crosses one of these dashed lines. The negative values are necessary to include the negative transitions mentioned in the previous section.

7. Discussion

The two techniques of tensorial expansion and eigenvalue correlation are useful in the construction and analysis of effective Hamiltonian models. The NITM is an efficient tool for incorporating tensor analysis, the Wigner–Eckart theorem and symmetry constraints.

In general, eigenvalues of an effective Hamiltonian are classified according to their behavior in different regions of the parameter ranges. The axial ESR spin Hamiltonian considered here is simple, but the correlation diagrams reveal the infinite field behavior of the spin states. It would be logical to study next the correlations for a nondiagonal $[\boldsymbol{H}']$ as, for example, in the case of a magnetic field at a nonzero angle to the high symmetry axis of an axial zero-field splitting term.

In fig. 2, the inverse Z mapping of the right-hand side region is an advantage in determining possible transitions at very high fields; however, it fails to give a realistic depiction of the splitting due to the compression of the high field values. Except for the $5/2 \rightarrow 7/2$ absorption, a linear plot would show that the spacing of the resonances with respect to the magnetic field (Z) is proportional to their zero-field splitting.

Otherwise, the correlation diagrams presented here have a number of advantages, including simplicity of graphing, ease of extrapolation and convenient application to specific models.

References

[1] Y. Tanabe and S. Sugano, J. Phys. Soc. Japan 9(1954)753–754.
[2] F.A. Matsen and M.L. Ellzey, Jr., J. Phys. Chem. 73(1969)2495.
[3] A. Abragam and B. Bleaney, *Electron Paramagnetic Resonance of Transition Metal Ions* (Oxford University Press, 1970).
[4] M.L. Ellzey, Jr., Croat. Chem. Acta 57(1984)1107.
[5] F.A. Matsen, private communication.
[6] H.J.A. Koopmans, Ph.D. Thesis. See also Phys. Stat. Sol. (b) 122(1984)317.
[7] J.S. Griffith, *The Theory of Transition Metal Ions* (Cambridge, 1961), p. 205.
[8] H.A. Buckmaster and R. Chatterjee, J. Chem. Phys. 83(1985)4001.
[9] M. Rotenberg, R. Bivins, N. Metropolis and J.K. Wooten, Jr., *The 3j and 6j Symbols* (MIT Press, Cambridge, MA, 1959).
[10] K.W.H. Stevens, Proc. Phys. Soc. 65(1952)209.
[11] H.A. Buckmaster, Can. J. Phys. 40(1962)1670.
[12] E.P. Wigner, *Group Theory* (Academic Press, 1959).